

**AUTHOR:**Abiodun Bayode<sup>1</sup> **AFFILIATION:**<sup>1</sup>School of Mechanical and Nuclear Engineering, North-West University, Potchefstroom, South Africa**CORRESPONDENCE TO:**

Abiodun Bayode

**EMAIL:**

reachabeyy@gmail.com

**DATES:**

Received: 13 May 2021

Revised: 28 Jan. 2022

Accepted: 02 Apr. 2022

Published: 29 Sep. 2022

**HOW TO CITE:**Bayode A. Surface finish, microhardness and microstructure of laser metal deposited 17-4PH stainless steel. S Afr J Sci. 2022;118(9/10), Art. #11152. <https://doi.org/10.17159/sajs.2022/11152>**ARTICLE INCLUDES:**

- 
- Peer review
- 
- 
- Supplementary material

**DATA AVAILABILITY:**

- 
- Open data set
- 
- 
- All data included
- 
- 
- On request from author(s)
- 
- 
- Not available
- 
- 
- Not applicable

**EDITOR:**

Michael Inggs

**KEYWORDS:**

additive manufacturing, dilution, martensite, microhardness, microstructure

**FUNDING:**

None



# Surface finish, microhardness and microstructure of laser metal deposited 17-4PH stainless steel

Laser metal deposition is a metal-based additive manufacturing technology. It is a very sensitive and complex process because of the different process parameters involved and the interrelations between these parameters. A thorough understanding of the underlying physics of the process is essential in developing a comprehensive database of the properties of materials processed with this technology. The main objective of this study was to investigate the effect of laser power on a laser-deposited 17-4 precipitation hardenable stainless steel alloy. The as-built microstructure, phase composition, microhardness and surface finish were analysed. The results show that a defect-free sample with good metallurgical bonding and minimal dilution can be produced using high laser power in the range 1400–2600 W and a scanning speed of 0.6 m/s. The microstructure in the clad layer was dominated by martensite and an improvement in surface finish and maximum hardness was observed with increased laser power.

**Significance:**

To fully benefit from the additive manufacturing technology, a comprehensive database of the material properties of alloys produced with this technology is required. This study expands on the body of knowledge related to the additive manufacturing of a 17-4PH stainless steel alloy, particularly highlighting the possibility of producing fully dense parts using higher laser power and scanning speed. These two parameters could significantly reduce the build time.

## Introduction

Additive manufacturing represents a variety of single-step fabrication technologies which produce near-net shape objects directly through the gradual addition of materials in layers from a three-dimensional computer model. Direct energy deposition and powder bed fusion are the most popular metal-based additive manufacturing methods. Laser metal deposition (LMD) is one of several additive manufacturing processes that are characterised as direct energy deposition systems. This technology is capable of fabricating fully dense metallic parts on a substrate with the aid of a high-power laser beam and powder delivery nozzle. LMD offers several benefits compared to traditional manufacturing systems, such as greater design flexibility which facilitates the production of complex-shaped parts with ease, thus enabling more innovative designs. It is a more sustainable manufacturing process as it allows for a more efficient use of materials because there is little or no material wastage or scraps. Furthermore, it enables microstructure enhancement through functional grading, and it can also be utilised for component repair. There are, however, several challenges associated with this technology such as slow built speed, which makes it more expensive and less attractive for mass productions, thus limiting its use to small batch and bespoke productions. Another important issue with additive manufacturing is the inability to reproduce components with microstructures identical to those obtained using traditional manufacturing methods. Other major drawbacks include porosity, residual stress, microstructure control, anisotropy, and dimensional accuracy.<sup>1-4</sup>

The main method of controlling the microstructure and mechanical properties as well as defects in LMD is through process parameter selection and optimisation. There are several processing parameters involved in LMD, of which laser power, scanning speed and powder flow rate are considered the most influential.<sup>5</sup> These parameters are interrelated, and their interactions have a strong influence on the final properties of parts, such that a small change in one parameter can result in significant changes in microstructure and mechanical properties. Consequently, it is imperative to understand the relationships between process parameters and optimal settings needed to obtain the desired material properties and effectively control the process to ensure reproducibility.

Martensitic precipitation hardening (PH) stainless steels such as 17-4PH are among the most common ferrous alloy increasingly processed by LMD. Besides its high strength and good corrosion resistance, this alloy has very good weldability which makes it suitable for additive manufacturing. Different microstructures and mechanical properties can be obtained depending on the heat treatment employed.<sup>6,7</sup> The highest hardness and strength are obtained after aging heat treatment with formation of coherent copper-rich precipitates. However, this alloy is not suitable for high temperature (above 300 °C) and very low temperature applications. 17-4PH is widely used in different industries such as chemical, medical, aerospace and metal forming to mention a few.<sup>8-10</sup> Several studies have been conducted to characterise the effect of processing conditions, powder characteristics and heat treatment on the evolving or resultant properties of this stainless steel alloy.<sup>11-24</sup> Most of the available studies are mostly focused on laser powder bed fusion technology. Thus, there is limited literature on the laser metal deposited 17-4PH. To this end, the main aim of this study was to generate a material database that will be useful in the manufacturing of 17-4PH parts. To achieve this aim, the objective was to evaluate the microstructure, microhardness and surface roughness of 17-4PH processed through LMD.

## Experimental procedure

17-4PH powder supplied by TLS Technik GmbH & Co was used in this study. According to the materials data sheet provided by the manufacturer, the powder particle size ranges from 45  $\mu\text{m}$  to 90  $\mu\text{m}$  with a mean of 70.56  $\mu\text{m}$ . The chemical composition of the powder is listed in Table 1. The substrate used was wrought AISI 316 plate with dimensions 100 x 100 x 10 mm<sup>3</sup>. The experiment was conducted using a high-power laser deposition system

consisting of a 2-kW ytterbium laser, a Kuka robotic arm, and a coaxial powder feeding system linked to a GTV PF 2/2 powder delivery system. Argon gas was used for both powder transport and for shielding during the deposition process. Samples were manufactured by varying the laser power whilst keeping other parameters constant. Laser power was varied between 1400 W and 2600 W. Beam diameter, scan speed, powder feed rate and overlapping rate were fixed at 2 mm, 0.6 m/s, 2 rev/min and 50% respectively. Table 2 shows the processing parameters used in this study.

**Table 1:** Chemical composition of the 17-4PH powder

Element	Fe	Ni	Cr	C	Mn	Cu	Si	Nb
Wt.%	Bal.	4.4	16.4	0.01	0.9	4	0.7	0.32

**Table 2:** Processing parameters used for manufacturing the specimens

Sample	Laser power (W)	Scan speed (m/min)	Beam diameter (mm)	Focal length (mm)	Overlap (%)
A1	1400	0.6	2	195	50
A2	1800				
A3	2200				
A3	2600				

After deposition, specimens for microstructural and microhardness observations were cross sectioned normal to the laser scanning direction. The coupons were prepared following standard metallographic procedure for stainless steel. Microstructure was analysed using an optical microscope (BX51M) after etching in Kallings no. 2 reagent for about 50 s and cleaning with acetone. A Rigaku Ultima IV X-ray diffractometer (XRD) equipped with CuK $\alpha$  radiation was used for phase identification. Microhardness analysis was conducted using a Vickers hardness tester by applying a load of 200 g for 15 s on the polished samples. A Hommel-Etamic Turbo Wave V7.53 was employed for surface roughness analysis. Each sample was analysed five times and the mean values of the roughness parameters ( $R_a$ ), ( $R_z$ ) and ( $R_{max}$ ) were documented. The measuring length, cut-off length, measurement range and probe speed used for analysis were 4.8 mm, 0.8 mm, 400  $\mu$ m and 0.50 mm/s, respectively.

## Results and discussion

### Powder characterisation

Figure 1 shows the morphology and XRD spectra of the powder. As can be seen from the scanning electron micrograph (Figure 1a), the powder is spherical in shape as is characteristic of gas atomised powder. Smaller particles or satellites can be observed coupled to larger particles. The XRD result presented in Figure 1b reveals a monophasic alloy which could be described as completely ferritic or martensitic or a combination of both. The lack of a clear description of the phases is due to the inability of most XRD equipment to differentiate between ferrite and martensite due to the minute difference in the lattice distortion between these two phases.<sup>22</sup> For this study, it was assumed to be martensitic.

### Microstructure and phase composition

The cross-section microstructure of the samples produced at different laser powers is shown in Figure 2. The samples appear structurally sound with no identifiable defects. It is clear from the images that increasing the laser power resulted in an increased melt pool depth. This was expected as the increase in laser power leads to a proportionate increase in specific energy density applied.<sup>25</sup> The average melt pool depth at the highest laser power (2600 W) was about 35.9  $\mu$ m. Furthermore, it was observed that the degree of undercutting or boundaries between adjacent tracks decreases with increase in laser power. The reason for this is that melt pool size increases as laser power increases, and when it reaches a certain critical size, it easily overlaps adjoining tracks.

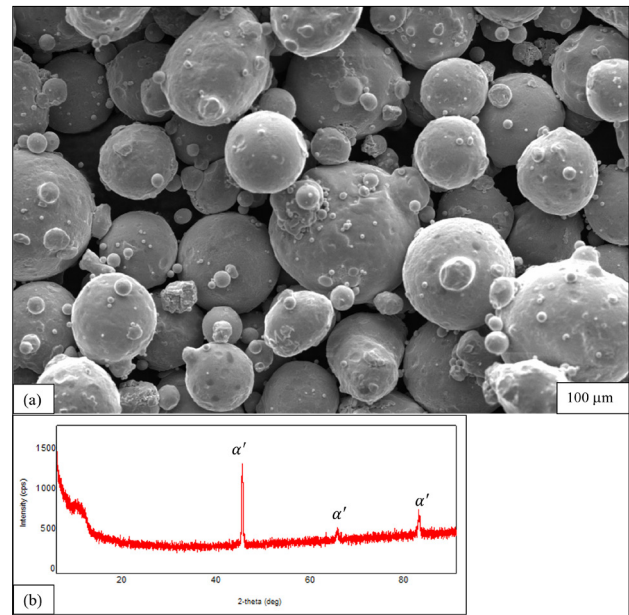


**Figure 1:** 17-4PH powder: (a) scanning electron micrograph and (b) X-ray diffraction spectrum.

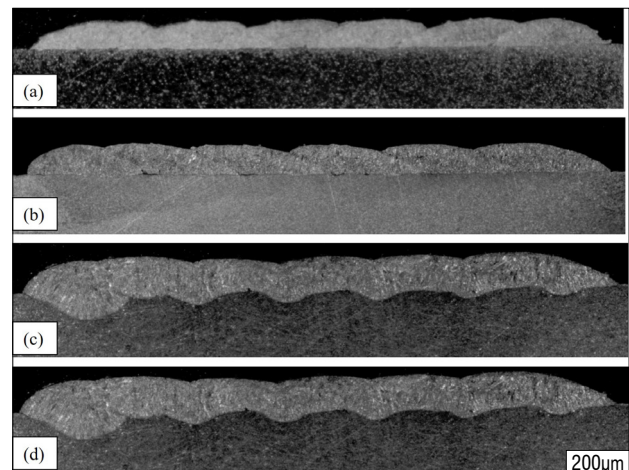


**Figure 2:** Overall view of samples: (a) A1, (b) A2, (c) A3, and (d) A4.

The microstructure of stainless steel alloys has significant impact on their mechanical properties, and it is common knowledge that alloy composition and manufacturing process employed can influence the final microstructure. Under equilibrium condition, the primary phase during solidification of 17-4PH is ferritic, which generally evolves as delta ferrite from the liquid phase, and, with further cooling, it transforms to austenite and then to martensite with traces of ferrite at ambient temperature. The chromium to nickel equivalent ( $C_{req}/N_{req}$ ) ratio is used to accurately predict the solidification behaviour of stainless steel alloys such as 17-4PH under equilibrium cooling.<sup>26</sup> However, at high cooling rates, the transformation kinetic is altered, resulting in a non-equilibrium solidification microstructure.<sup>27</sup> This is a major reason why the microstructure observed for wrought 17-PH stainless steel differs from that of comparable additive manufactured 17-4PH alloy. For example, 17-4PH alloy processed via conventional methods such as casting tends to have a fully martensitic microstructure<sup>7,28</sup>, whereas different microstructures (mostly a combination of martensite and austenite) have been reported for additive manufactured 17-4PH<sup>4,15,22,29</sup>. Various factors, such as processing atmosphere and high cooling rates in the range  $10^5$ – $10^6$  K/s in LMD can lead to the formation of fine grains and the stabilisation or retention of austenite.<sup>4,15,27</sup>

Figure 3a–d presents the optical micrograph of the clad zone of the various samples fabricated by varying laser power. All the specimens display a very fine microstructure distinctive of additive manufacturing.<sup>23</sup>

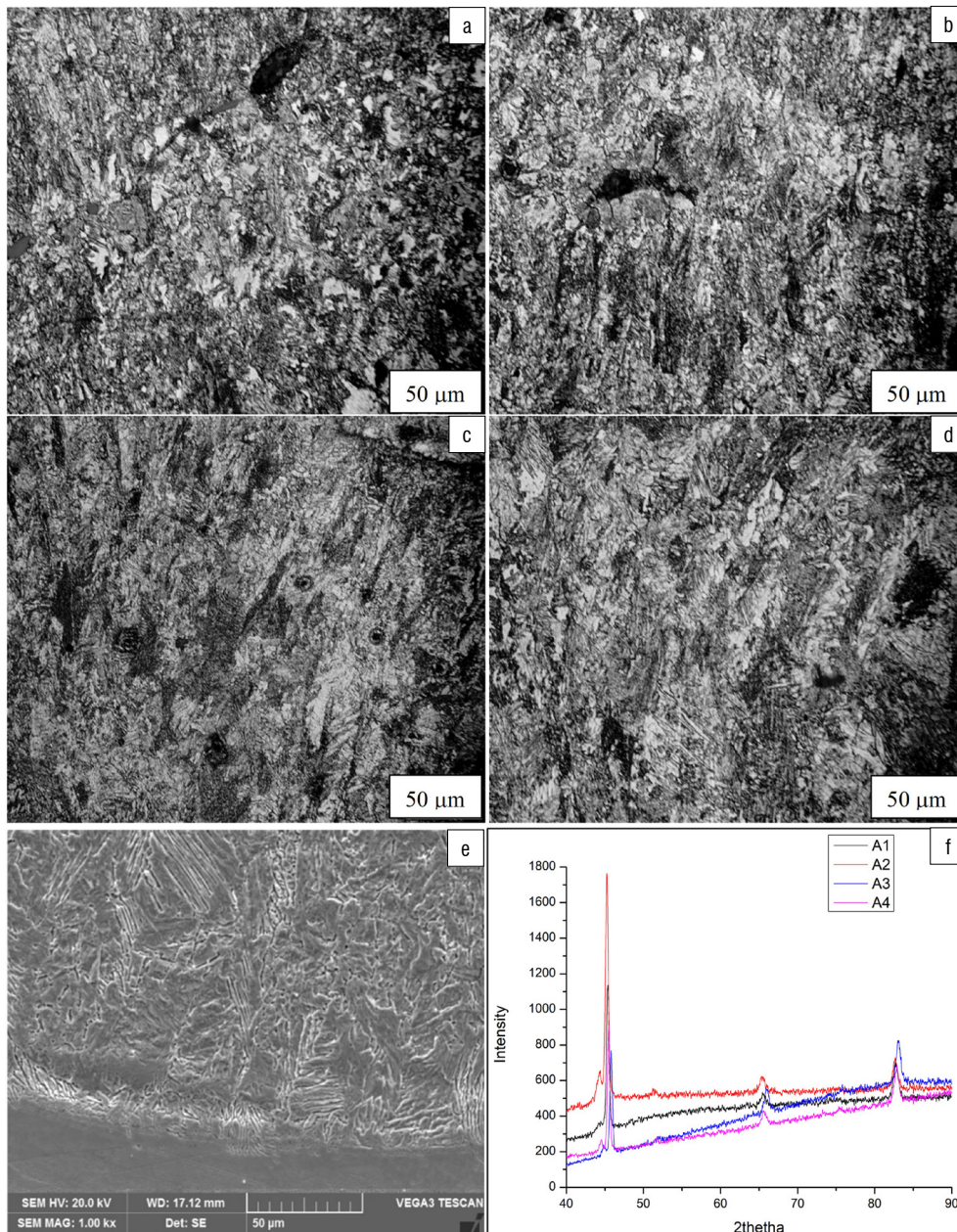


**Figure 3:** (a–d) Optical images of samples A1, A2, A3, and A4, respectively; (e) scanning electron micrograph of A2; and (f) X-ray diffraction spectra of specimens produced at different laser powers.

The microstructure is composed predominately of martensite with some retained austenite. The martensite morphology is not discernible from the optical micrographs, mainly due to the etchant used. A lathy martensite is expected because of the low carbon content of 17-4PH powder used.<sup>30</sup> Increasing the laser power appears to have resulted in some slight refinement of grains. That is, the coarsening of grains was induced as laser power increased. Furthermore, it has been observed that increasing the laser power causes a reduction in cooling rate which can induce carbon segregation and also affects the size and shape of martensite formed<sup>31</sup>, both of which impact steel strength. Figure 3e shows a higher magnification scanning electron micrograph of the interface of Sample A2. As can be seen, the grain structure is characterised by fine columnar grains which grew epitaxially from the substrate along the temperature gradient. The substrate acts as a heat sink. The limited changes in microstructure observed could be attributable to the low laser interaction time resulting from the very high scan speed and laser power used for manufacturing.

XRD analysis of the top horizontal plane was conducted to determine phase composition. By comparing the XRD spectra of the starting powder

(Figure 1a) and fabricated specimen (Figure 3f), it is clear that the LMD process has resulted in changes in phase composition. The LMD samples are not entirely composed of martensite as observed in the precursor powder, but also contain austenite – albeit in small quantity. As can be seen, martensite has a higher peak intensity compared to the austenitic phase. Sample A2 shows a higher peak intensity in comparison with the other samples; there is, however, no clear trend with respect to laser power and phase composition. The presence of austenite, even in small quantities, can have a significant impact on mechanical properties because it is a weaker phase. No copper precipitates were detected in any of the samples, which is not unusual as it is rarely observed in the as-printed state, but more commonly observed after aging hardening. Lastly, the XRD spectra for the LMD specimens suggest grains grew preferentially along the easy growth directions. In general, the result of the phase composition analysis is consistent with the optical microscopy observation and the literature.<sup>23</sup>

### **Microhardness and surface roughness**

Figure 4 shows the microhardness profile as a function of laser power. As expected, there was an upward trend in hardness from the bottom to

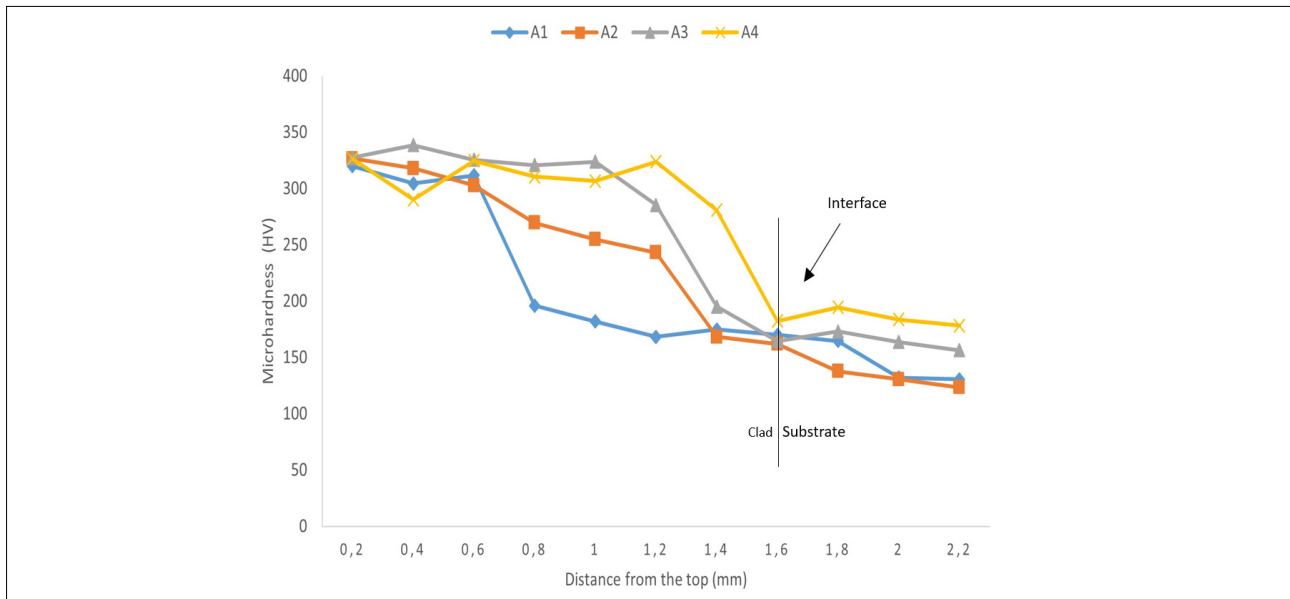


**Figure 4:** Effect of laser power on microhardness.

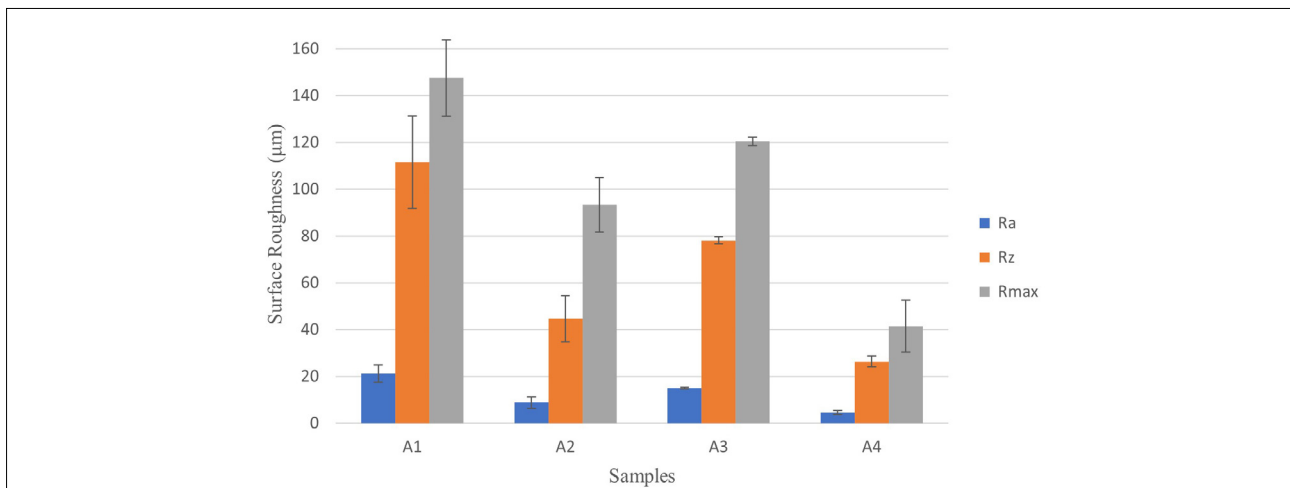


**Figure 5:** Effect of laser power on surface roughness.

the top surface. It can be observed that the maximum hardness increased with the increase in laser power. Sample A1 produced with the lowest laser power had the lowest maximum hardness (319 HV) and was also the least homogeneous in terms of overall hardness. On the other hand, Sample A4 had the highest maximum hardness of about 331.5 HV which is almost on par with wrought 17-4PH stainless steel (322–350 VHN) but much lower than hardness values that have been reported for laser deposited 17-4PH which can get as high as 371–400 HV.<sup>24</sup> The changes in microhardness can be attributed to grain refinement produced by laser power variation. This result is in agreement with that of a similar study conducted on the selective laser melting of 17-4PH.<sup>32</sup>

The average surface roughness parameters are presented in Figure 5. As Figure 5 shows, there is an inverse correlation between the laser power and the surface roughness. Increasing the laser power resulted in a decrease in surface roughness, except for a laser power of 2200 W (Sample A3). The enhancement in surface quality can be ascribed to a larger molten pool created as well as the better melting efficiency obtained at higher laser power. The lowest average roughness was obtained when the laser power was set to 2600 W, giving  $R_a$ ,  $R_z$  and  $R_{max}$  values of 4.53  $\mu\text{m}$ , 26.36  $\mu\text{m}$ , and 41.46  $\mu\text{m}$ , respectively. Furthermore, based on the standard deviations of the surface roughness parameters – specifically the  $R_a$  values, it appears that a somewhat more homogeneous surface is obtained with increasing laser power.

## Conclusion

The objective of this study was to investigate the influence of laser power on a laser deposited 17-4PH alloy. The following are some of the pertinent conclusions of this work as it relates to the goal of the research.

17-4PH stainless steel powder was successfully deposited on the 316 austenitic stainless steel substrates at three different laser power settings ranging between 1400 W and 2200 W. All the samples produced were crack free, fully dense and with extremely low dilution.

Microscopy and XRD analysis revealed a predominantly martensitic/ferritic microstructure with some retained austenite. The grain structure of the as-built samples can be described as composed of fine columnar dendrites. The XRD analysis of the samples shows the occurrence of two different phases dominated by martensite, and also suggests the component is characterised by a crystallographic texture.

The microhardness evaluation indicates a direct relationship between laser power and maximum microhardness. Furthermore, increasing the laser power resulted in a decrease in surface roughness. However, a more homogeneous surface roughness was observed at a laser power of 2200 W.

## Competing interests

I have no competing interests to declare.

## References

1. Herzog D, Seyda V, Wycisk E, Emmelmann C. Additive manufacturing of metals. *Acta Mater.* 2016;117:371–392. <https://doi.org/10.1016/j.actamat.2016.07.019>
2. Kok Y, Tan XP, Wang P, Nai MLS, Loh NH, Liu E, et al. Anisotropy and heterogeneity of microstructure and mechanical properties in metal additive manufacturing: A critical review. *Mater Des.* 2018;139:565–586. <https://doi.org/10.1016/j.matdes.2017.11.021>
3. Zhang B, Li Y, Bai Q. Defect formation mechanisms in selective laser melting: Defect formation mechanisms in selective laser melting: A review. *Chin J Mech Eng.* 2017;30: 515–527. <https://doi.org/10.1007/s10033-017-0121-5>
4. Murr LE, Martinez E, Hernandez J, Collins S, Amato KN, Gaytan SM, et al. Microstructures and properties of 17-4 PH stainless steel fabricated by selective laser melting. *J Mater Res Technol.* 2012;1(3):167–177. [https://doi.org/10.1016/s2238-7854\(12\)70029-7](https://doi.org/10.1016/s2238-7854(12)70029-7)
5. Mahmood RM. Processing parameters in laser metal deposition process. In: *Laser metal deposition process of metals, alloys, and composite materials: Engineering materials and processes.* Cham: Springer; 2018. p. 61–92. [https://doi.org/10.1007/978-3-319-64985-6\\_4](https://doi.org/10.1007/978-3-319-64985-6_4)
6. Murayama M, Katayama Y, Hono K. Microstructural evolution in a 17-4 PH stainless steel after aging at 400 °C. *Metall Mater Trans A Phys Metall Mater Sci.* 1999;30(2):345–353. <https://doi.org/10.1007/s11661-999-0323-2>
7. Sun Y, Hebert RJ, Aindow M. Effect of heat treatments on microstructural evolution of additively manufactured and wrought 17-4PH stainless steel. *Mater Des.* 2018;156:429–440. <https://doi.org/10.1016/j.matdes.2018.07.015>
8. Sabooni S, Chabok A, Feng SC, Blaauw H, Piiper TC, Yang HJ, et al. Laser powder bed fusion of 17-4 PH stainless steel: A comparative study on the effect of heat treatment on the microstructure evolution and mechanical properties. *Addit Manuf.* 2021;46, Art. #102176. <https://doi.org/10.1016/j.addma.2021.102176>
9. Murr LE, Martinez E, Hernandez J, Collins S, Amato KN, Gaytan SM, et al. Microstructures and properties of 17-4 PH stainless steel fabricated by selective laser melting. *J Mater Res Technol.* 2012;1(3):167–177. [https://doi.org/10.1016/S2238-7854\(12\)70029-7](https://doi.org/10.1016/S2238-7854(12)70029-7)
10. Lo KH, Shek CH, Lai JKL. Recent developments in stainless steels. *Mater Sci Eng R Rep.* 2009;65(4–6):39–104. <https://doi.org/10.1016/j.mser.2009.03.001>
11. Makoana N, Yadroitsava I, Möller H, Yadroitsev I. Characterization of 17-4PH single tracks produced at different parametric conditions towards increased productivity of LPBF systems – The effect of laser power and spot size upscaling. *Metals.* 2018;8(7), Art. #:475. <https://doi.org/10.3390/met8070475>
12. Bayode A, Pityana S, Akinlabi ET, Shongwe MB. Effect of scanning speed on laser deposited 17-4PH stainless steel. In: *Proceedings of the 8th International Conference on Mechanical and Intelligent Manufacturing Technologies; 2017 February 03–06; Cape Town, South Africa.* IEEE; 2017. p. 1–5. <https://doi.org/10.1109/icmimt.2017.7917404>
13. Mahmoudi M, Elwany A, Yadollahi A, Thompson SM, Bian L, Shamsaei N. Mechanical properties and microstructural characterization of selective laser melted 17-4 PH stainless steel. *Rapid Prototyp J.* 2017;23(2):280–294. <https://doi.org/10.1108/rpj-12-2015-0192>
14. Pasebani S, Ghayoor M, Badwe S, Irrinki H, Atre SV. Effects of atomizing media and post processing on mechanical properties of 17-4 PH stainless steel manufactured via selective laser melting. *Addit Manuf.* 2018;22:127–137. <https://doi.org/10.1016/j.addma.2018.05.011>
15. Vunnam S, Saboo A, Sudbrack C, Starr TL. Effect of powder chemical composition on the as-built microstructure of 17-4 PH stainless steel processed by selective laser melting. *Addit Manuf.* 2019;30, e100876. <https://doi.org/10.1016/j.addma.2019.100876>
16. LeBrun T, Nakamoto T, Horikawa K, Kobayashi H. Effect of retained austenite on subsequent thermal processing and resultant mechanical properties of selective laser melted 17-4 PH stainless steel. *Mater Des.* 2015;81:44–53. <https://doi.org/10.1016/j.matdes.2015.05.026>
17. Yadollahi A, Shamsaei N, Thompson SM, Elwany A, Bian L. Effects of building orientation and heat treatment on fatigue behavior of selective laser melted 17-4 PH stainless steel. *Int J Fatigue.* 2017;94:218–235. <https://doi.org/10.1016/j.ijfatigue.2016.03.014>
18. Gu H, Gong H, Pal D, Rafi K, Starr T, Stucker B. Influences of energy density on porosity and microstructure of selective laser melted 17-4PH stainless steel. Paper presented at: 24th International SFF Symposium – An Additive Manufacturing Conference; 2013 August 12–14; Austin, TX, USA. <http://dx.doi.org/10.26153/tsw/15572>
19. Hsu TH, Huang PC, Lee MY, Chang KC, Lee CC, Li MY, et al. Effect of processing parameters on the fractions of martensite in 17-4 PH stainless steel fabricated by selective laser melting. *J Alloys Compd.* 2021;859, Art. #157758. <https://doi.org/10.1016/j.jallcom.2020.157758>
20. Giganto S, Martínez-Pellitero S, Barreiro J, Zapico P. Influence of 17-4 PH stainless steel powder recycling on properties of SLM additive manufactured parts. *J Mater Res Technol.* 2022;16:1647–1658. <https://doi.org/10.1016/j.jmrt.2021.12.089>
21. Steponavičiūtė A, Selskienė A, Stravinskis K, Borodinas S, Mordas G. 17-4 PH stainless-steel as a material for high resolution laser metal deposition. *Mater Today Proc.* 2021;52(4):2268–2272. <https://doi.org/10.1016/j.matpr.2021.08.143>
22. Sun Y, Hebert RJ, Aindow M. Effect of heat treatments on microstructural evolution of additively manufactured and wrought 17-4PH stainless steel. *Mater Des.* 2018;156:429–440. <https://doi.org/10.1016/j.matdes.2018.07.015>
23. Zai L, Zhang C, Wang Y, Guo W, Wellmann D, Tong X, et al. Laser powder bed fusion of precipitation-hardened martensitic stainless steels: A review. *Metals.* 2020;10(2), Art. #255. <https://doi.org/10.3390/met10020255>
24. Mathoho I, Akinlabi ET, Arthur N, Tlotleng M, Makoana NW. The effects of LENS process parameters on the behaviour of 17-4 PH stainless steel. In: *Proceedings of the 149th Annual Meeting & Exhibition Supplemental Proceedings; 2020 February 23–27; San Diego, CA, USA.* Cham: Springer; 2020 p. 481–490. [https://doi.org/10.1007/978-3-030-36296-6\\_45](https://doi.org/10.1007/978-3-030-36296-6_45)
25. Levy GN, Schindel R, Kruth JP. Rapid manufacturing and rapid tooling with layer manufacturing (LM) technologies, state of the art and future perspectives. *CIRP Annals.* 2003;52(2):589–609. [https://doi.org/10.1016/s0007-8506\(07\)60206-6](https://doi.org/10.1016/s0007-8506(07)60206-6)
26. Kotecki DJ, Siewert TA. WRC-1992 constitution diagram for stainless steel weld metals: A modification of the WRC-1988 diagram refined constitution diagram offers more accurate FN prediction for Cu-containing stainless steels and dissimilar metal joints. *Welding J.* 1992;71(5):171–178. [https://doi.org/10.1016/0261-3069\(93\)90110-h](https://doi.org/10.1016/0261-3069(93)90110-h)
27. Kou S. Solidification and liquation cracking issues in welding. *JOM.* 2003;55(6):37–42. <http://dx.doi.org/10.1007/s11837-003-0137-4>
28. Ziewiec A, Zielińska-Lipiec A, Tasak E. Microstructure of welded joints of X5CrNiCuNb 16-4 (17-4 PH) martensitic stainless steel after heat treatment. *Arch Metall Mater.* 2014;59(3):965–970. <http://dx.doi.org/10.2478/amm-2014-0162>
29. Yadollahi A, Shamsaei N, Thompson SM, Elwany A, Bian L. Mechanical and microstructural properties of selective laser melted 17-4PH stainless steel. In: *Proceedings of the ASME 2015 International Mechanical Engineering Congress and Exposition; 2015 November 13–19; Houston, TX, USA.* New York: American Society of Mechanical Engineers; 2016. <https://doi.org/10.1115/imece2015-52362>
30. Krauss G. *Steels: Processing, structure, and performance.* 2 ed. Materials Park, OH: ASM International; 2015. p. 495–534.
31. Eggbauer (Vieweg) A, Ressel G, Gruber M, Prevedel P, Marsoner S, Stark A, et al. Different cooling rates and their effect on morphology and transformation kinetics of martensite. In: *Stebner AP, Olson GB, editors. Proceedings of the International Conference on Martensitic Transformations; Chicago.* Cham: Springer; 2018. p. 35–40. [https://doi.org/10.1007/978-3-319-76968-4\\_6](https://doi.org/10.1007/978-3-319-76968-4_6)
32. Cheng Z, Kwok CT, Lo KH. Laser surface melting of 17-4 PH precipitation-hardenable stainless steel. In: *Proceedings of the 4th Pacific International Conference on Applications of Lasers and Optics; 2010 March 23–25; Wuhan, China.* Orlando, FL: Laser Institute of America; 2010. p. 1203. <http://dx.doi.org/10.2351/1.5057183>